Fabrication a controlled-release pesticide for improving UV-shielding properties and reducing toxicity via coating polydopamine

Ya Wang
Hunan Agricultural University
Chaonan Li
Hunan Agricultural University
Xing Zhang
Hunan Agricultural University
Wei Chen
Hunan Agricultural University
Ying Zhang
Hunan Agricultural University
Xiaogang Li (lxgang@hunau.edu.cn)
Hunan Agricultural University https://orcid.org/0000-0002-2380-5245

Research article

Keywords: Pyraclostrobin, Polydopamine, UV-shielding properties, Sustained release, Bioactivity, Acute toxicity evaluation

Posted Date: June 16th, 2020

DOI: https://doi.org/10.21203/rs.3.rs-28348/v1

Abstract

In modern agriculture, controlled-release formulations (CRF) is greatly desirable for achieving valid utilization and loss reduction of pesticides. It can also alleviate the adverse effect on non-target organism. In this study, we used PDA as a depositing layer, constructed pyraclostrobin@SiO 2 @polydopamine microcapsule (Pyr@SiO 2 @PDA MC). The resulting microcapsule is a near-rod shape (about 1.152μm), which has a drug-loading efficiency of 55%. FT-IR and TG analysis revealed the successful entrapment of the pesticide. The microencapsulation had important function in the slow-release rate of the pyraclostrobin and superior UV-shielding properties. Moreover, bioactivity of the microcapsule against Fusarium oxysporum f.sp.vasinfectum was determined and it exhibited better inhibition activity than pyraclostrobin technical in the later stage. At last, acute toxicity tests demonstrated that Pyr@SiO 2 @PDA MC on zebrafish with lower toxicity on the first day. These results showed that Pyr@SiO 2 @PDA MC may process broader application potential in agriculture.

Introduction

Pyraclostrobin (Fig. 1) is a methoxy acrylate fungicide developed by BASF in 1993 [1]. It acts on the cytochrome bcl complex in the fungal mitochondrial respiratory chain, preventing electron transfer and inhibiting mitochondrial respiration, making mitochondria unable to produce the energy (ATP) required for normal metabolism of cells, leading to cell death [2,3].Pyraclostrobin (pyr) has a very broad bactericidal spectrum with protective and therapeutic effects on crops [4]. There is, however, a high ecological safety risk when used in paddy fields, which restricts the application of pyraclostrobin to a certain extent [5,6]. A viable strategy to reducing the accumulation of pesticides in a water environment is to develop controlled release formulations (CRFs). Li fabricated pyr microcapsules (MCs) with Fe^{3+} and tannic acid, which showed excellent effcacy on rice blast and signifcantly lower toxicity to four model organisms [7]. However, the drug loading of the microcapsules is not mentioned in this manuscript, and we cannot know the loading capacity of the carrier for pyraclostrobin. In addition, the preparation process needs to rely on the chelation of calcium lignosulfonate molecules with Fe^{3+} to prepare a pre-film and then perform a second film formation, which is cumbersome.

Controlled release technology (CRT) has been extensively employed in industries and fields such as pharmaceuticals, coatings, cosmetics, etc [8–12]. In the field of pesticide formulation processing, CRT is also an ideal choice to advance the efficiency of pesticides and reduce environmental pollution. Therefore, it has become an important direction for the development of new pesticide formulation [13–15]. To date, a host of inorganic materials like SiO_2, and various polymers are used as a carrier to deliver the drug in order to achieve controlled-release [16–18]. Study on silica has attracted a wide range of attentions due to its prominent properties, such as facile preparation, low cost, polymer coatings, etc [19–21]. More importantly, it has a significant impact on enhancing plant tolerance against biotic and abiotic stresses [22]. These advantages make it an ideal and suitable choice for drug delivery in agriculture.

Dopamine (Da), which can form an adherent polydopamine (PDA) coating in a weakly alkaline solution through oxidative self-polymerization [23]. In addition, PDA coating can also be used for other reactions because of its abundant functional groups (amino, imino, and catecholyl) [24,25]. Xin prepared a PDA coated avermectin microcapsules (Av@PDA MC) with prominent sustained-release performance and good adhesion properties [26]. Gao fabricated a novel imidacloprid microcapsule with PDA followed by PU exhibited excellent dispersion stability [27]. Undeniably, PDA is considered to be a promising pesticide encapsulant for obtaining novel controlled release formulation [28–30].

Microcapsules are one of the microparticulate systems which have shown tremendous potential and are used for controlled-release formulation and to improve the environment security and persistence of agrochemicals [31,32]. Pesticide microcapsules made of reliable material as carrier could increase length of activity as well as reduce side effects on the environment. In the present work, a simple method has been attempted to encapsulate pyr for acquiring high drug-loading efficiency. The preparation of our microcapsules and the drug loading process are performed simultaneously to obtain Pyr@SiO_2 MC. This can effectively improve the preparation efficiency. The deposition of PDA on the surface can give microcapsules excellent UV shielding properties. Prepared Pyr@SiO_2@PDA MC was characterized on physicochemical properties including size, morphology, drug loading, release behavior and UV-shielding. The bactericidal activities againsted *Fusarium oxysporum f.sp.vasinfectum* as well as the acute toxicity to zebrafish were also investigated.

Experimental Section

Materials

Pyraclostrobin technical (97% TC) was provided by Jiangsu Subin Agrochemical Co., Ltd (Jiangsu China). 250g/L Pyraclostrobin emulsifiable concentrate (EC) was purchased from BASF (Germany). Dopamine hydrochloride(DA) and Tris-HCl(1.5M, pH = 8.8) were supplied by Beijing solarbio science&technology Co., Ltd. Cetyl trimethyl ammonium bromide (CTAB) and tetraethyl orthosilicate (TEOS) were purchased from Aladdin reagent (Shanghai) co., Ltd. Ethyl acetate, tween–80 emulsifier, methanol and the other reagents were came from Sinopharm group chemical reagent co. Ltd and used as received without further purification. The chemicals what we used for the experiments were of analytical grade.

Preparation of Pyr@SiO_2@PDA microcapsule

Microcapsules were prepared as reported by literature with some modification [33]. Firstly, 0.5% w/v water phase was obtained by dissolving 0.5g cetyl trimethyl ammonium bromide in 100.0mL of deionized water. Next, 0.5g Pyr was dissolved in a mixture ethyl acetate and tetraethyl orthosilicate to prepare oil phase. Then, the oil phase was mixed with the aforementioned water solution, ammonia water (25%–28%, v/v) was added dropwise to adjust its pH to 8. The mixture was agitated in a magnetic stirrer (C-MAG HS 7, IKA Company, Germany) with the rotation speed 600rpm for 2h, placed at room temperature

overnight. Subsequently, DA and 200μl Tris-HCl was added and stirred at room temperature for 24h (Fig. 2). After centrifugation, the solution was washed at least three times with deionized water and dried under vacuum at 45°C. The dried sample was named as Pyr@SiO_2@PDA MC. In order to obtain the highest loading content of pyr, different amount of DA were used to prepare the microcapsules (Table 1).

Characterization of the Pyr@SiO_2@PDA microcapsules

Particle size of Pyr@SiO_2@PDA MC was measured by Mastersizer 2000 (Malvern instruments Ltd., Britain). The particles were suspended in deionized water for measurement, and each sample was measured three times. The appearance of the sample was observed by a JMS - 6360 scanning electron microscope (SEM; Tokyo, Japan) at 25 KV. Nicolet-IS 5 (United States) was used to record the characteristic absorption peak of the products in range of 4000–500 cm^{-1} at room temperature. For purpose of confirming the existence of the Pyr and determine loading ratio, thermogravimetric analysis (TG) was conduced over the temperature range from 25 to 600 ◦C at 10 ◦C/min rate by mean of Mettler Toledo thermal analyzer (TGA 2). Zeta potential was tested by micro-electrophoresis apparatus (JS94H2 Shanghai Zhongchen Digtal Technology Apparatus Co., Ltd., China). Equation 1 was utilized to calculate the effective components in the microcapsule [34]. Samples containing the same quality of Pyr, including Pyr TC, Pyr@SiO_2 MC, Pyr@SiO_2@PDA MC were enclosed in quartz tube. Ultraviolet (UV) light was selected as light source, with the irradiance of 3.00 mW/cm^2, rated power of 1.5 W × 2, at a distance of 15 cm, and set the dark control. Sampling was performed at 1, 2, 4, 8 and 10h, respectively. The released amounts of Pyr were monitored by HPLC (Agilent Technologies Inc., America) and the photodegradation rate of samples was calculated according to Equation (2).

$$\text{Drug loading}(\%) = \frac{\text{Mass of loaded drugs (mg)}}{\text{Mass of weighted microcapsule (mg)}} \times 100 \quad (1)$$

$$\text{Photodegradable rate}(\%) = \frac{\text{Residue under dark condition} - \text{Residue under light condition}}{\text{Residue under dark conditio}} \times 100 \quad (2)$$

In vitro release studies

The drug-loaded microcapsule was placed in a dialysis bag (MWCO 3500 Da) and immersed in 200.0 mL of release medium(phosphate buffer saline, ethanol and tween–80 emulsifier, 140:59:1 v/v/v), maintaining the temperature at 25±1◦C. Some of the solution was withdrawn at appropriate intervals for

the HPLC assay, and the same amount of fresh release medium was added after each sampling at predetermined time intervals to keep a constant volume. Meanwhile, for the control study, 97% Pyr TC was used as a reference under the same condition.

Indoor virulence assay

Fungicidal activity of Pyr@SiO_2@PDA MC was assessed by the growth rate method using *Fusarium oxysporum f.sp.vasinfectum* as the tested strain, and the 250g/L Pyr EC was used as a control dosage form [35]. The tested strain was isolated and purified by the Laboratory of Pesticide Science, College of Plant Protection, Hunan Agricultural University. Firstly, the medicament was formulated into five concentrations of drug-containing medium at a concentration of 5, 10, 50, 100, and 200 mg/mL. Subsequently, the fungicidal evaluation under the first, third, fifth, seventh, and ninth days was then performed. Finally, the cross method was applied to determin the colony diameter, and the concentration for 50% of maximal effect (EC_{50}) was calculated according to the formula (3). The control group was treated with sterile water of the same volume, each treatment was performed at least in triplicate.

$$\text{Mycelium groth inhibitin rate}(\%) = \frac{\text{Control group colony growth diameter} - \text{Treatment group colony growth diamter}}{\text{Control group colony growth diameter}} \times 100 \quad (3)$$

Acute toxicity tests on Zebrafish

In order to evaluate the acute toxicity of the sample to aquatic organisms, zebrafish, which respond quickly and inexpensively, was used as a model organism. The zebrafish was the same as the zebrafish used in the previous experiments [36], purchased from a commercial supplier in Changsha China, weighing 0.2 to 0.4g and having an average length of 2.0 to 3.0cm. Acute toxicity tests were carried out according to guideline for “environmental safety evaluation tests of chemical pesticides standards" [37]. The zebrafish were carried out in accordance with the basic principles of animal experiments at Hunan Agricultural University, and were approved by the Pesticide Chemistry Laboratory of the College of Plant Protection.

Acute toxicity studied were performed in a 96h semi-static test [38,39]. Briefly, placed 10 tails of adult fish in 3.00 L aerated water with diverse concentrations of agents(Pyr@SiO_2@PDA MC and Pyr EC) ranging from 0.02 to 0.12 mg/L. Control experiments with only aerated water were consistent with the test group. Three repetitions were set for each experiment. Keep room temperature at 25±1°C and light/dark cycle (16 hr light/8 hr dark) constant. Dead fish being removed in order to avoid affecting the test. With SPSS, software available in computer, LC_{50}values and their 95% confidence limits could be obtained at 24, 48, 72, and 96 h, respectively.

Results And Discussion

Effect of dopamine addition on microcapsules

The particle size of microcapsules increased with the addition of DA, but decreased when DA increased to 80mg (Table 1).This may be due to the limited specific surface area that can be contacted by the microcapsule. As the covered PDA reaches an extreme value, increasing the dosage of DA, particle size will not continue to increase. Besides, the drug load will first increase and then decline with the increase of DA. When the addition amount of DA was 40mg, the drug load could reach 55%, which was higher than the single- and double-shelled cyhalothrin/SiO_2 microcapsules (about 50.0% and 25.0%, respectively) [40]. As depicted in Figure 3a, the color of the solution gradually deepens with the increase of DA. After tableting, samples S1, S2 and S3 were grayish white, grayish black and dark gray, respectively (Fig. 3b). The color of microcapsule samples became darker with the increase of DA content.

Characterization of samples

Samples S1, S2 and S3 were examined under different magnifications. The microstructure of the microcapsule is built on rod-like structure coated by PDA. Altered levels of DA showed different degrees of agglomeration. When the content of DA increased from 10mg to 20mg, the dispersion of the particles could be effectively improved and the coating effect of the PDA could be better seen (Figs. 4a-f). After adding more DA to the particles, the rod-like structure of the particles is destroyed and agglomeration occurs. In this case, the obtained particles visibly presented irregular shape (Figs. 4g-i). Finally, combining the results of drug loading and SEM, S2 (in Table 1) was selected for further study.

TG and DTG analysis of SiO_2@PDA MC and Pyr@SiO_2@PDA MC in nitrogen atmosphere have been carried out to further vertify the presence of the pry. As shown in Fig. 5a, TG analysis was also carried out for quantitative analysis. The curves of SiO_2@PDA MC and Pyr@SiO2@PDA MC showed weight loss in the range of 300–600 ∘C due to the decomposition of PDA [41]. A new weight loss started at about 200 ∘C, which was assigned to the decomposition of pyr. The weight loss of bare SiO_2@PDA MC was about 15%, but that of Pyr@SiO_2@PDA MC ascended to 73%. Therefore the weight of pyr loaded in the samples was about 58%. It also illustrated the successful encapsulation of pyr in the Pyr@SiO_2@PDA MC. The calculation found that the drug loading rate was only 55%, which was significantly lower than that obtained by TG analysis (58%). This may be because despite grinding and ultrasound, the samples were not completely destroyed and some drugs were not completely released, resulting in a low calculated drug loading rate.

Zeta potential was used to monitor the change of particle potential before and after PDA coating. Potential beginning with the silica was −16.05 mV and turned to −20.11 mV after the deposit of PDA layer (shown in Fig.6). Since the Pyr@SiO_2 MC have a large amount of Si-OH groups, the zeta potential values appeared to be negative at first, and when the PDA is coated, the PDA also has a large amount of -

OH and -NH showing negative zeta potetntial so that the negative potential of the particle band increases [42]. Zeta potential values shifted with the cladding of the PDA layers, which indicated the successfully deposition of the PDA.

IR Spectrum Analysis

The infrared spectroscopy of DA, PDA, SiO_2, Pyr@SiO_2 MC and Pyr@SiO_2@PDA MC were performaned by FTIR spectra, which were utilized to verify successful encapsulation of pesticide. DA had many narrow peaks, which were characteristic of small molecule (Fig. 7a); while PDA showed only a few main peaks: the main peak of the aromatic ring was about 1623 cm^{-1}, and the main peak of the catechol-OH group was about 3446 cm^{-1} [43]. In the FTIR spectra of the microcapsule, the main peaks of SiO_2 and PDA overlapped with that of the Pyr (Fig. 7b). The infrared spectrum of the SiO_2 exhibited a typical peak at 1100 cm^{-1}(Si-O-Si) corresponding to the primary silica bonds [44]. Compared with SiO_2, the characteristic absorption peak of drug-loaded microcapsules appeared at 1717 cm^{-1}, which was attributed to the stretching vibration of C = O in Pyr. Besides, a peak corresponding to the stretching vibration of Si-O-Si appeared at 1100 cm^{-1}. The characteristic absorption peak from Pyr@SiO_2@PDA MC (3446 cm^{-1}) appeared as a wider peak of -OH groups compared to Pyr@SiO_2 MC. The results stated that Pyr was encapsulated into the microcapsule. What's more,no new IR peaks indicated no chemical reactions occurred [45].

Studies of the UV-shielding properties of the PDA layer for Pry

Statistically, plenty of applied pesticides are lost due to hydrolysis and photolysis [46]. Effectively encapsulation can protect the active ingredients and prolonging the duration [47]. The UV-shielding properties of the PDA carrier was studied in ethanol/water solution with different samples. Fig. 8 hows the photolysis curves of Pyr TC, Pyr@SiO_2 MC and Pyr@SiO_2@PDA MC. In the first two hours, the photolysis rates of the microcapsules were close to each other. After 4h of UV illumination, the photodegradation rate of TC was nearly 50%, while those of the Pyr@SiO2 MC and Pyr@SiO2@PDA MC were 22.10% and 18.66% respectively. The photodegradation rate of Pyr TC, Pyr@SiO_2 MC were 2.2 times and 1.5 times than that of Pyr@SiO_2@PDA MC after 12h of illumination. These results clearly showed that the PDA carrier had remarkable UV shielding properties, which can significantly reduce the photodegradation rate of Pyr and improve its stability. In addition, Tong [48] found that GO with PDA layer had obvious adhesion properties. When PDA coating was added, the persistence of pesticides on cucumber leaves was improved after simulated rain-wash test. Therefore, PDA carrier was an ideal carrier to extend the service life of pesticides.

Drug Release Property

The cumulative release curves of Pyr from the TC and Pyr@SiO_2@PDA MC are shown in Figure 9 After 12 h immersed in phosphate buffer saline, the cumulative release rate of Pyr from TC was more than 35% w/w, compared to 10% w/w when loaded in microcapsule (Fig.9a). After 24h, the Pyr released from TC was over 80% w/w; however, the obtained microcapsule released less than 15% w/w of Pyr after 24h immersed, and 38% w/w after 192h. The cumulative release of the Pyr from TC is up to 98% w/w after 192h. It seems that Pyr@SiO_2@PDA MC liberated much lesser Pyr molecules at the same period. Result revealed that the active ingredients from Pyr@SiO_2@PDA MC was released slowly in vitro and the diffusion time was longer. Due to the presence of the PDA coating, the microcapsule was a good option for controlling the long-term release of the Pyr, which also helped to extend the duration.

Fungicidal activity of Pyr@SiO_2@PDA microcapsule

With sufficiently demonstrated characterization of the Pyr@SiO_2@PDA MC in size, morphology, IR and release property, we began to study its bactericidal activity. The results of the indoor virulence test are set out in the table 2. At the test concentration, Pyr@SiO_2@PDA MC was significantly inferior to the EC in inhibiting the growth of mycelium. On the fifth day after the administration, the fungicidal activity of microcapsule was similar to that of the EC. Very interestingly, the EC_{50} values of MC and EC at ~9d post administration were 5.62 and 85.11 mg/mL, respectively. The former is about 15 times more toxic than the latter. With the extension of time, the active ingredients are continuously released in the microcapsule while are gradually decomposed in the EC. Thus, the virulence of the microcapsule gradually surpassed that of the EC, showing a very obvious sustained release effect.

Toxicity Evaluation

During the experiment, no death or abnormal behavior was detected in the blank control group of zebrafis. In contrast, the death has begun in the treatment group on the first day. At the beginning, after contact with the high-concentration EC, the zebrafish immediately turned upside down, swam rapidly, and jumped out of the water. Subsequently, poisoned zebrafish reacted dull and the swimming speed was slow. When fish died, their abdomen and cheeks turned reddish (Fig. 10)

The LC_{50} values for 24–96h and their 95% confidence limits were expressed in Table 3. LC_{50} values of Pyr EC and Pyr@SiO_2@PDA MC in 24h were 0.065 and 0.118 mg/L. The value of LC_{50} was between 0.1 mg a.i./L and 1 mg a.i./L. Thus, according to guideline for “environmental safety evaluation tests of chemical pesticides standard” (GB/T 31270.12–2014), virulence of MC on zebrafish was high toxicity. While the Pyr EC was extreme toxicity(LC_{50}≦0.1 mg a.i./L). The toxicity of MC to zebrafish was lower in the first 48h compared with Pyr EC (Table 3). This indicated that effective encapsulation can reduce the toxicity of pesticides to non-target organisms to some extent. This conclusion was similar to the result reported

by Xu. He used poly(2-dimethylaminoethylmethacrylate) (PDMAEMA) and chitosan (CS) fabricated CS-g-PDMAEMA microcapsules. LC_{50} (24h) values of Pyr@CS-g-PDMAEMA were 0.1020 mg/L, which was less toxic than the control [49]. While, in the next 48 h, the acute toxicity of MC against zebra fish became comparable with that of Pyr EC. LC_{50} (96 h) values of Pyr EC and Pyr@SiO_2@PDA MC were 0.049 and 0.062 mg/L, respectively.

Conclusion

In this work, we have fabricated the Pyr@SiO_2@PDA microcapsule in a straightforward way. The pyr-loaded microcapsules with maximum drug loading of 55% demonsrated sustained release for up to 200 hours. Contrasting with free pyr, PDA could effectively improve the photostability of pesticides under ultraviolet light. It comes up with an effective strategy for protecting such photounstable pesticide. The obtained microcapsule processes longer duration against *Fusarium oxysporum f.sp.vasinfectum* compared to traditional formulation (250g/L Pyr EC). On the other hand, a reduction in the amount of pesticide used helps to alleviate environmental pollution. Moreover, microcapsulation could provide a degree of protection against zebrafish on the first 24 h. Consequently, this formulation could enhance utilization efficiency while exert less unintended negative effects on environment. Therefore, successful development of Pyr@SiO_2@PDA microcapsule has made it possible to improve its application properties.

Declarations

Ethics declarations

Consent statement

The experimental animal programs involved in this experiment were carried out in accordance with the basic principles of animal experiments at Hunan Agricultural University, and were approved by the Pesticide Chemistry Laboratory of the College of Plant Protection.

Competing interests

The authors declare that they have no competing interests.

Funding

This work was funded by the National Key Research and Development Program, Special Research and Development of Fertilizers and Pesticides (Yfd0201200, 2016).

Acknowledgments

The author would like to thank all the authors for their guidance and help with the experiment. Thanks to the Hunan Agricultural University Testing Center for characterization of the materials.

Data availability

All data generated during this study are included in this published article and additional data will be shared upon request to the corresponding author.

Contributions

WY designed the study; WY and LCN performed the experiments and wrote the manuscript; ZX, CW and ZY analysed the data. All authors read and approved the final manuscript.

Abbreviations

Pry: pyraclostrobin

PDA: polydopamine

MC : microcapsule

FT-IR: Fourier transform infrared spectroscopy

TG: Thermogravimetric Analysis

CRFs: controlled release formulations

CRT: controlled release technology

Da: dopamine

Av: avermectin

PU: polyuria

EC: emulsifiable concentrate

CTAB: cetyl trimethyl ammonium bromide

TEOS: tetraethyl orthosilicate

TC: technical

EC_{50}: concentration for 50% of maximal effect

LC_{50}: lethal concentration 50

HPLC: High Performance Liquid Chromatograph

SEM: scanning electron microscope

References

1 Patel, J. S., et al., 2012. Pyraclostrobin sensitivity of baseline and fungicide exposed isolates of Pyrenophora tritici-repentis. Crop Protetion, 34, 37–41.

2 Yin, Y. N., et al., 2012. Molecular characterization of pyraclostrobin resistance and structural diversity of the cytochrome b gene in Botrytis cinerea from apple. Phytopathology, 102(3), 315–22.

3 Karadimos, D. A., et al., 2005. Biological activity and physical modes of action of the Qo inhibitor fungicides trifloxystrobin and pyraclostrobin against Cercospora beticola. Crop Protection, 24(1), 23–29.

4 Myresiotis, C. K., et al., 2008. Baseline Sensitivity of\r, Botrytis cinerea\r, to Pyraclostrobin and Boscalid and Control of Anilinopyrimidine- and Benzimidazole-Resistant Strains by These Fungicides. Plant Disease, 92(10), 1427–1431.

5 Cusaac, J. P. W., et al., 2015. Terrestrial exposure and effects of Headline AMP?Fungicide on amphibians. Ecotoxicology, 24(6), 1341–1351.

6 Cabrera, A., et al., 2014. Influence of biochar amendments on the sorption–desorption of aminocyclopyrachlor, bentazone and pyraclostrobin pesticides to an agricultural soil. Science of The Total Environment, 470–471, 438–443.

7 Li, B. X., et al., 2017. Using coordination assembly as the microencapsulation strategy to promote the efficacy and environmental safety of pyraclostrobin. Advanced Functional Materials, 1701841.

8 Fang, Y., et al., 2015. Biointerfaces, Enhanced cellular uptake and intracellular drug controlled release of VESylated gemcitabine prodrug nanocapsules. Collolds Surf B Biointerfaces, 128, 357–362.

9 Thonggoom, O., et al., 2016. In vitro controlled release of clove essential oil in self-assembly of amphiphilic polyethylene glycol-block-polycaprolactone. Journal of Microencapsulation, 1–10.

10 Reguera-Nuñez, E., et al., 2014. Implantable controlled release devices for BMP–7 delivery and suppression of glioblastoma initiating cells. Biomaterials, 35(9), 2859–2867.

11 Siepmann, F., et al., 2008. Polymer blends for controlled release coatings. Journal of Controlled Release, 125(1), 1–15.

12 Martins, I. M., et al., 2014. Microencapsulation of essential oils with biodegradable polymeric carriers for cosmetic applications. The Chemical Engineering Journal, 245(6), 191–200.

13 Peppas, N. A., and Langer, R. J. S., 1994. New challenges in biomaterials. Science 263, 1715–1720.

14 Cheng, G., et al., 2018. A user-friendly herbicide derived from photo-responsive supramolecular vesicles. Nature Communications, 9(1), 2967–2979.

15 Nuruzzaman, M., et al., 2016. Nanoencapsulation, Nano-Guard for Pesticides: A New Window for Safe Application. Journal of Agricultural and Food Chemistry, 64(7), 1447–1483.

16 Wibowo, D., et al., 2014. Sustained release of fipronil insecticide in vitro and in vivo from biocompatible silica nanocapsules. Journal of Agricultural and Food Chemistry, 62(52), 12504–12511.

17 Chunli, X. and Lidong, C., 2018. Synthesis and Characterization of Stimuli-Responsive Poly(2-dimethylamino-ethylmethacrylate)-Grafted Chitosan Microcapsule for Controlled Pyraclostrobin Release. International Journal of Molecular Sciences, 19(3), 854–867.

18 Feng, R., et al., 2013. Novel star-type methoxy-poly(ethylene glycol) (PEG)–poly(ε-caprolactone) (PCL) copolymeric nanoparticles for controlled release of curcumin. Journal of Nanoparticle Research, 15(6), 1748–1759.

19 Barik, T. K., et al., 2008. Nanosilica—from medicine to pest control. Parasitology Research, 103(2), 253–258.

20 Battegazzore, D., et al., 2014. Rice husk as bio-source of silica: preparation and characterization of PLA–silica bio-composites. RSC Advances, 4(97), 54703–54712.

21 Ciriminna, R.,et al., 2013. The sol–gel route to advanced silica-based materials and recent applications. Chemical reviews, 113(8), 6592–6620.

22 Mody, V. V., et al., 2014. Magnetic nanoparticle drug delivery systems for targeting tumor. Applied Nanoscience, 4(4), 385–392.

23 Toma, M., et al., 2014. Flexible Teflon Nanocone Array Surfaces with Tunable Superhydrophobicity for Self-Cleaning and Aqueous Droplet Patterning. ACS Applied Materials & Interfaces, 6(14), 11110–11117.

24 Zhang, L., et al., 2011. Bioinspired preparation of polydopamine microcapsule for multienzyme system construction. Green Chemistry, 13, 300–306.

25 Dong, Z., et al., 2014. Bio-inspired surface-functionalization of graphene oxide for the adsorption of organic dyes and heavy metal ions with a superhigh capacity. Journal of Materials Chemistry A, 2(14), 5034–5040.

26 Jia, X., et al., 2014. Adhesive polydopamine coated avermectin microcapsules for prolonging foliar pesticide retention. ACS Applied Materials & Interfaces, 6(22), 19552–19558.

27 Gao, Z., et al., 2017. Preparation and characterization of a novel imidacloprid microcapsule via coating of polydopamine and polyurea. RSC advances, 7(26), 15762–15768.

28 Lynge, M. E., et al., Polydopamine—a nature-inspired polymer coating for biomedical science, Nanoscale, 3, 4916–4928.

29 Liu, Y., et al., 2018. A physically crosslinked polydopamine/nanocellulose hydrogel as potential versatile vehicles for drug delivery and wound healing. Carbohydrate Polymers, 188, S014486171830119X.

30 Luo, R., et al., 2013. Huang, Improved immobilization of biomolecules to quinone-rich polydopamine for efficient surface functionalization. Collolds Surf B Biointerfaces, 106, 66–73.

31 Zhang, W., et al., 2014. Preparation and characterization of novel functionalized prochloraz microcapsules using silica-alginate-elements as controlled release carrier materials. ACS Applied Materials & Interfaces, 6, 11783–11790.

32 Kumar, S., et al., 2014. Synthesis, characterization and on field evaluation of pesticide loaded sodium alginate nanoparticles. Carbohydrate Polymers,101, 1061–1067.

33 Liang, Y., et al., 2017. Development of novel urease-responsive pendimethalin microcapsules using silica-ipts-pei as controlled release carrier materials, ACS Sustainable Chemistry & Engineering, 5, 4802–4810.

34 Jyothi, N. V. N., et al., 2010. Microencapsulation techniques, factors influencing encapsulation efficiency. Journal of Microencapsulation, 27(3), 187–197.

35 Sarah, G., et al., 2017. Silver Oxide Coatings with High Silver-Ion Elution Rates and Characterization of Bactericidal Activity. Molecules, 22, 1487–1502.

36 Wang, Y., et al. 2018. Compound Pesticide Controlled Release System Based on the Mixture of poly (butylene succinate) and PLA. Journal of Microencapsulation, 1–33.

37 General Administration of Quality Supervision, Inspection and Quarantine of the People's Republic of China. China National Standardization Managementcommittee, Part 12: Fish Acute Toxicity Test, the Test Guidelines on Environmental Safety assEssment for Chemical Pesticides (GB/T 31270.12–2014)

38 Calazans., et al. 2013. Assessment of toxicity of dissolved and microencapsulated biocides for control of the Golden Mussel Limnoperna fortunei. Marine Environmental Research, 91, 104–108.

39 Wang. X., et al., 2015. Hepatic oxidative stress and catalyst metals accumulation in goldfish exposed to carbon nanotubes under different pH levels. Aquatic Toxicology, 160, 142–150.

40 Xu. Y., et al., 2015, Preparation and characterization of single- and double-shelled cyhalothrin microcapsules based on the copolymer matrix of silica–N-isopropyl acrylamide–bis-acrylamide, Rsc Adv, 5(65):52866–52873.

41 S. Zhang, Y. Zhang, G. Bi, J. Liu, Z. Wang, Q. Xu, H. Xu and X. Li, J. Hazard. Mater., 2014, 270, 27–34

42 Xiong, W., et all., 2016, Multifunctional Plasmonic Co-Doped Fe2O3 @polydopamine-Au for Adsorption, Photocatalysis, and SERS-based Sensing, Particle & Particle Systems Characterization, 33(9), 602–609.

43 Fei, B., et al., 2008. Coating carbon nanotubes by spontaneous oxidative polymerization of dopamine, Carbon, 46(13), 1795–1797.

44 Gu, S., et al., 2013. A detailed study of the effects of pyrolysis temperature and feedstock particle size on the preparation of nanosilica from rice husk. Industrial Crops and Products, 50, 540–549.

45 Mattos, B. D. and Magalhães, W. L. E., 2016. Biogenic nanosilica blended by nanofibrillated cellulose as support for slow-release of tebuconazole. Journal of Nanoparticle Research, 18(9), 274–283.

46 Xuan, R. C., et al., 2010. Hydrolysis and photolysis of oxytetracycline in aqueous solution. Journal of Environmental Science & Health Part B, 45(1), 73–81.

47 Ghormade, V., et al., 2011. Perspectives for nano-biotechnology enabled protection and nutrition of plants. Biotechnology Advances, 29(6), 792–803.

48 Tong, Y, J., et al., 2018. Adhesive and Stimulus-Responsive Polydopamine-Coated Graphene Oxide System for Pesticide-Loss Control. Journal of Agricultural & Food Chemistry, 66, 11, 2616–2622.

49 Xu, C. L., et al., 2018. Synthesis and characterization of stimuli-responsive poly(2-dimethylamino-ethylmethacrylate)-grafted chitosan microcapsule for controlled pyraclostrobin release. International Journal of Molecular Sciences, 19(3), 854–867.

Table

Table 1 Composition of the microcapsule prepared for carrying purposes

Sample	DA (mg)	Particle size (μm)	Loading efficiency (%)
S1	20	1.126±0.13	50.21±0.23
S2	40	1.152±0.24	55.00±0.41
S3	80	0.980±0.14	53.38±0.66

Note: Results are reported as mean ± SD (n = 3)

Table 2 The result of indoor toxicity determination of pyraclostrobin EC and Pyr@SiO2@PDA MC against Fusarium oxysporum f.sp.vasinfectum

Tested agents	Investigation time (d)	Equation $y=$	EC_{50} value (mg/mL) r	Related coefficient (R)
pyraclostrobin emulsifiable concentrate (EC)	1	4.794+1.032*x*	0.58±0.07	0.946
	3	4.168+1.008*x*	6.76±0.38	0.957
	5	3.698+0.909*x*	26.9±0.75	0.983
	7	3.357+0.992*x*	45.32±0.91	0.975
	9	3.228+0.885*x*	85.11±1.21	0.976
$Pyr@SiO_2$@PDA microcapsule (MC)	1	3.285+0.876*x*	91.20±1.34	0.986
	3	3.149+1.115*x*	46.24±0.85	0.954
	5	3.955+0.816*x*	19.05±0.52	0.960
	7	3.672+1.298*x*	10.47±0.47	0.995
	9	3.973+1.366*x*	5.62±0.42	0.981

Note: Results are reported as mean ± SD (n = 3).

Table 3. Acute toxic effects of microsphere to zebrafish

Agents	Time (h)	Toxicity equation (y=)	Correlation (R^2)	LC_{50} (a.i. mg/L)	95%confidence limits (a.i. mg /L)
pyraclostrobin emulsifiable concentrate (EC)	24	4.050+3.800x	0.961	0.065±0.017	0.053-0.089
	48	4.392+3.655x	0.919	0.063±0.015	0.047-0.099
	72	3.915+3.169x	0.902	0.058±0.012	0.037-0.125
	96	2.368+1.802x	0.960	0.049±0.010	0.042-0.057
Pyr@SiO_2@PDA microcapsule (MC)	24	2.213+2.382x	0.986	0.118±0.028	0.097-0.157
	48	2.992+2.888x	0.978	0.092±0.026	0.081-0.124
	72	2.987+2.539x	0.993	0.067±0.013	0.059-0.077
	96	3.238+2.685x	0.977	0.062±0.011	0.056-0.070

Note: Results are reported as mean ± SD (n = 3). The a.i. in the table represented available ingredient.

Figures

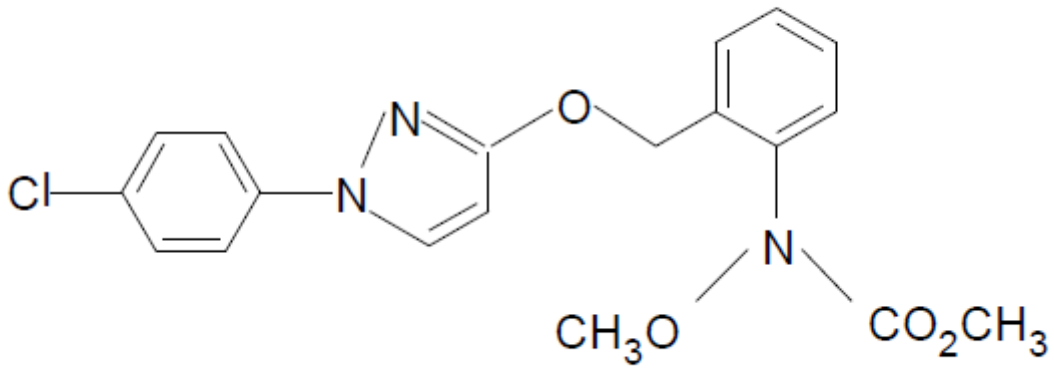

Figure 1

Structural formula of pyraclostrobin

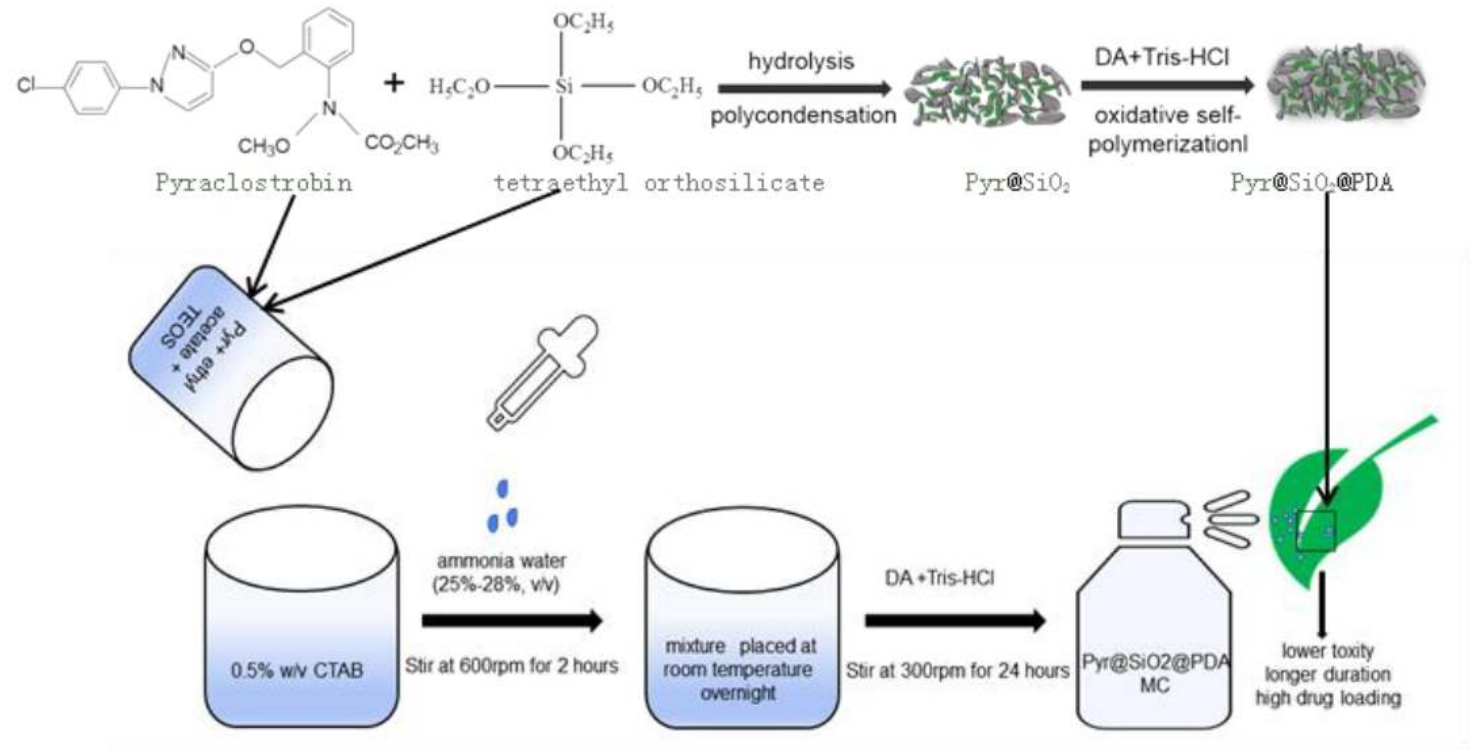

Figure 2

The preparation process of Pyr@SiO2@PDA MC

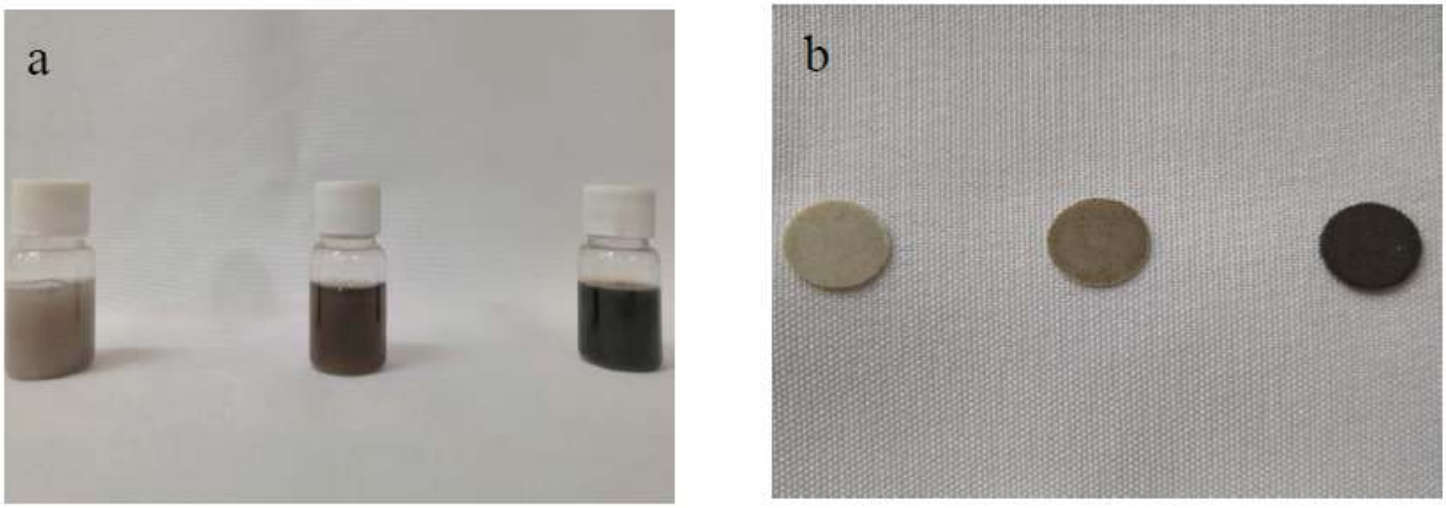

Figure 3

Microcapsule samples with different DA before centrifugation (a) and after tablettin (b)

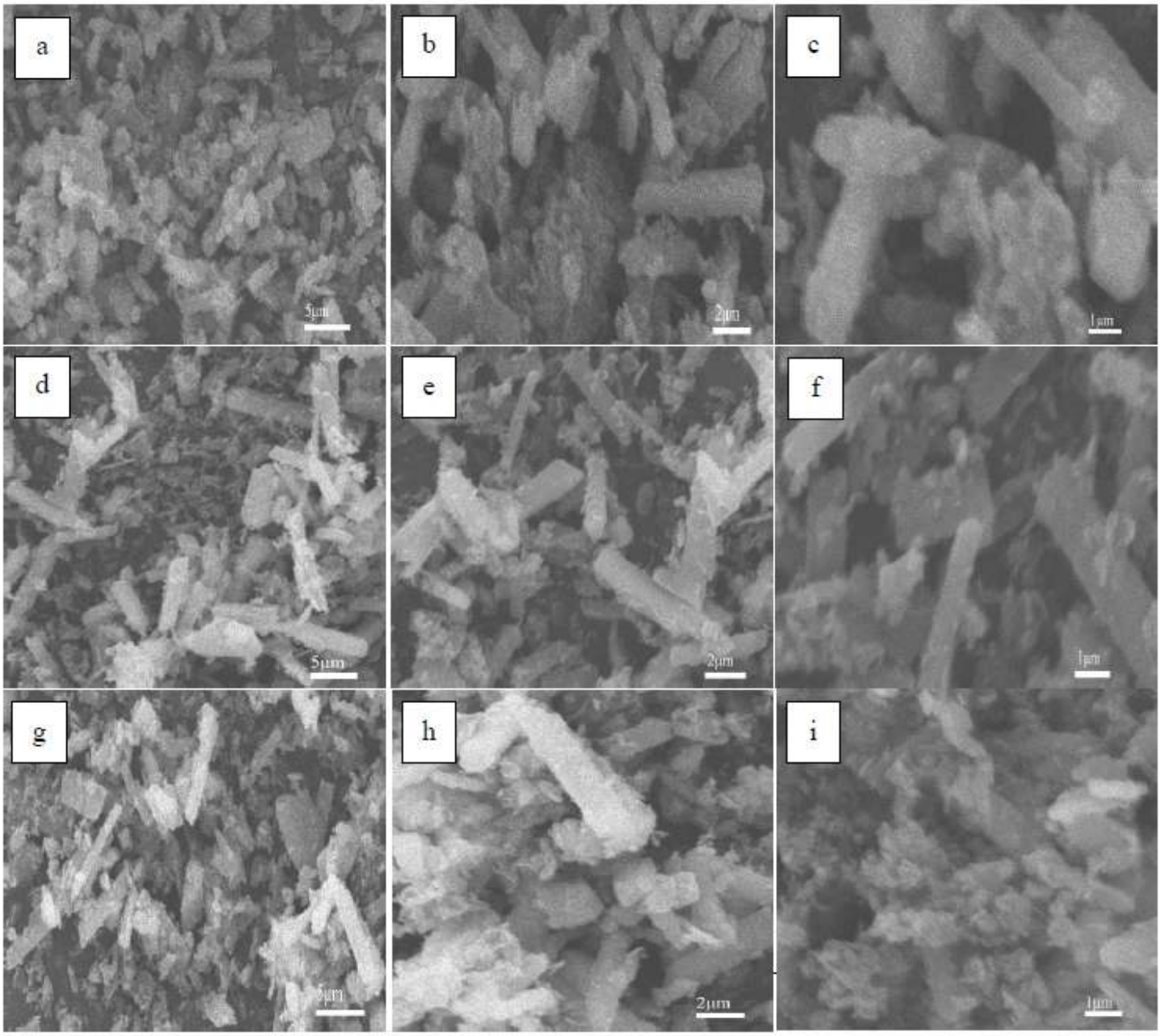

Figure 4

SEM images of microcapsule samples with different content of DA (a S1×1000, b S1×2000, c S1×5000, d S2×1000, e S2×2000, f S2×5000, g S3×1000, h S3×2000, i S3×5000)

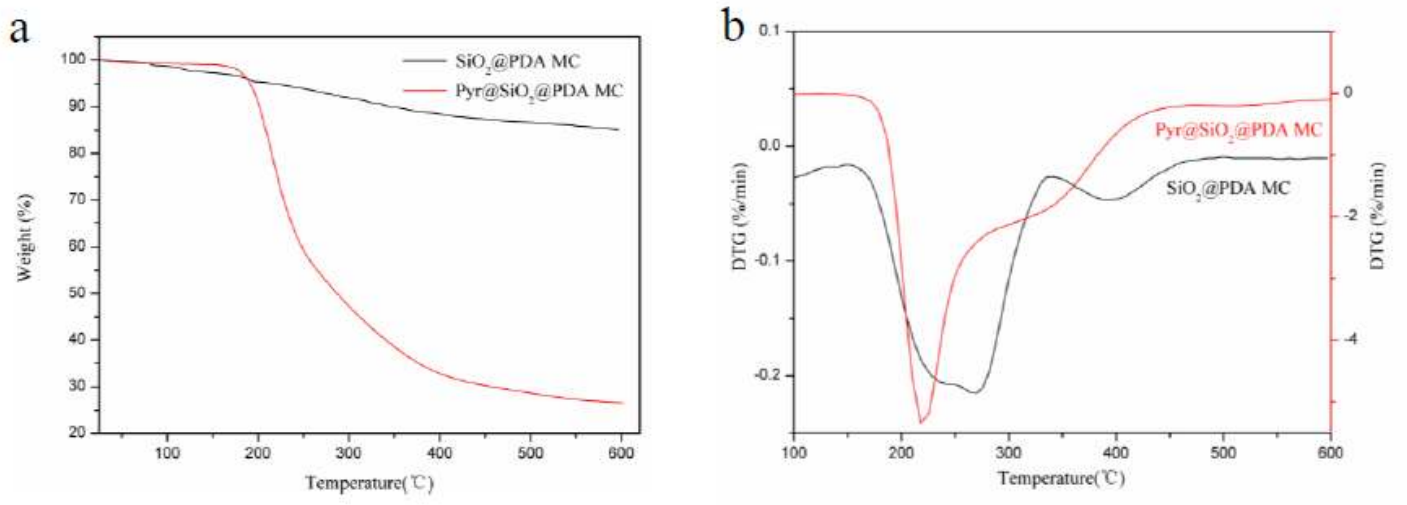

Figure 5

TG and DTG curves for SiO2@PDA MC and Pyr@SiO2@PDA MC

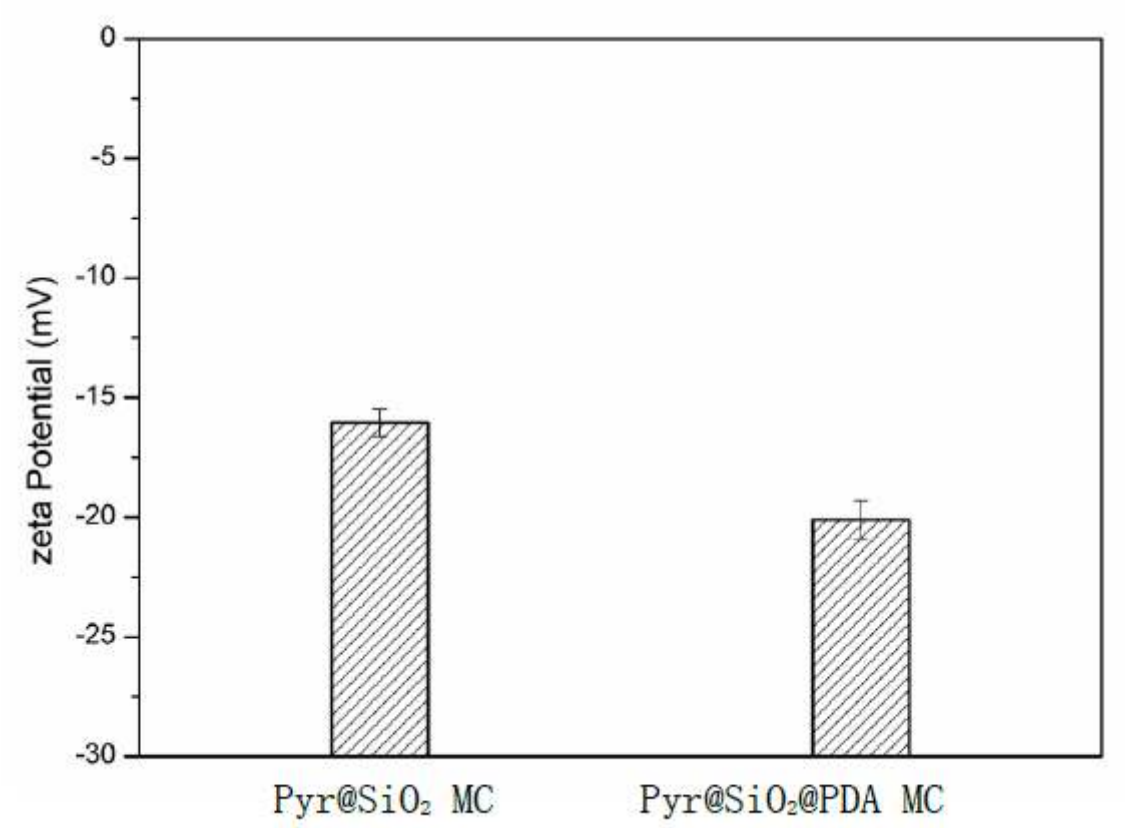

Figure 6

Zeta potential of Pyr@SiO2 MC and Pyr@SiO2@PDA MC

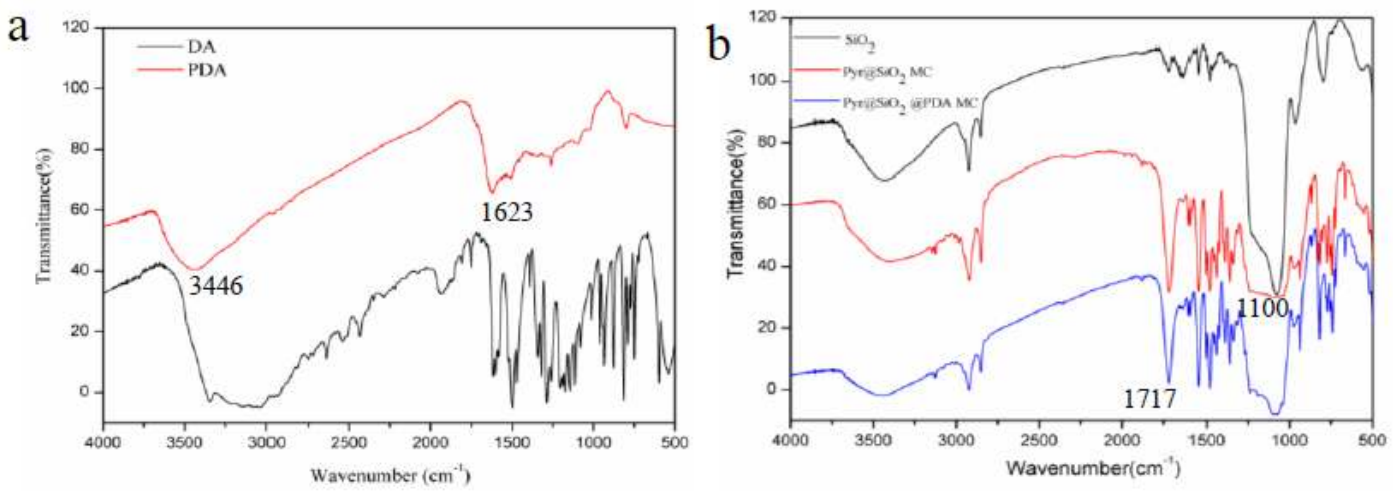

Figure 7

FTIR spectra (a) of DA and PDA, (b) of SiO2, Pyr@SiO2 MC and Pyr@SiO2@PDA MC

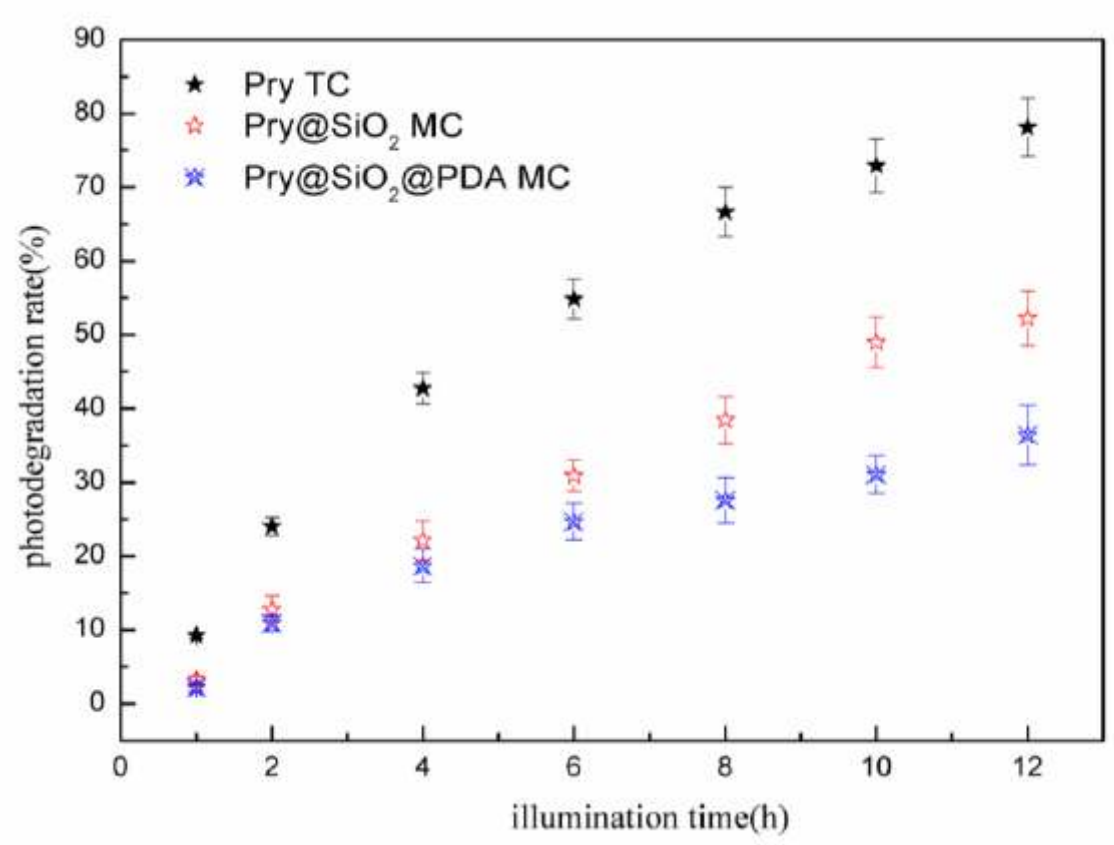

Figure 8

Photolysis curve of Pyr TC, Pyr@SiO2 MC and Pyr@SiO2@PDA MC

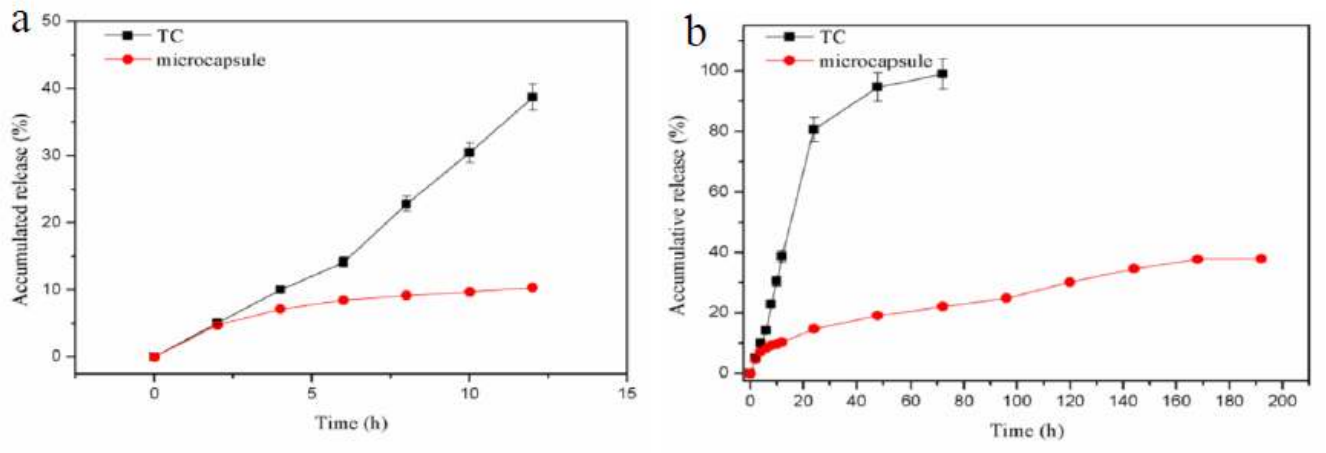

Figure 9

Profiles of Pyr release from TC and Pyr@SiO 2 @PDA MC along 12 h (a) and 192 h (b)

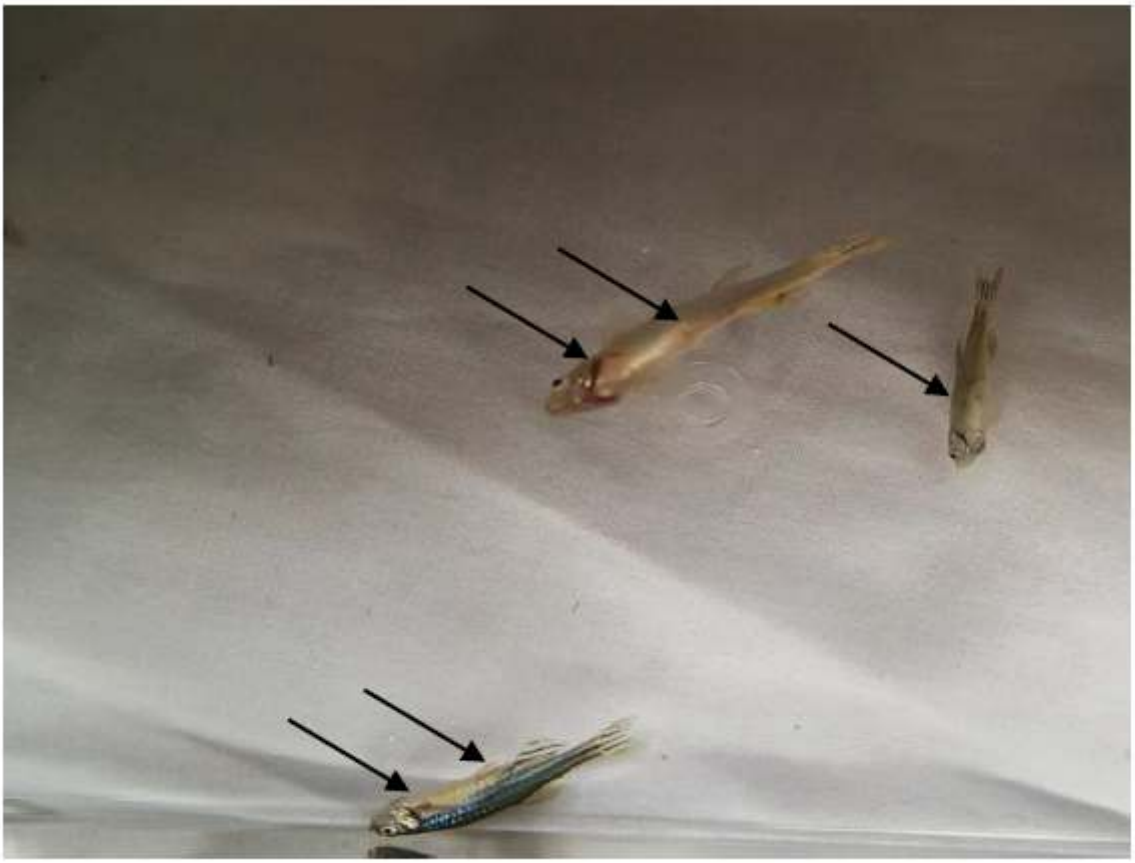

Figure 10

A few small red granular (As indicated by the arrow on the diagram) deposit s in dead zebrafish.

Supplementary Files

This is a list of supplementary files associated with this preprint. Click to download.

- GraphicalAbstractforreview.docx